engineering proceedings

MDPI

Proceeding Paper

Simulation-Based Design and Analysis for MEMS Vibrating Ring Gyroscope †

Waqas Amin Gill *, Ian Howard, Ilyas Mazhar and Kristoffer McKee *

Department of Mechanical Engineering, Curtin University, Perth, WA 6845, Australia
* Correspondence: waqasamin.gill@postgrad.curtin.edu.au (W.A.G.); k.mckee@curtin.edu.au (K.M.)
† Presented at the 4th International Electronic Conference on Applied Sciences, 27 October–10 November 2023; Available online: https://asec2023.sciforum.net/.

Abstract: Microelectromechanical system (MEMS) inertial sensors are integral components in a variety of smart electronic devices, most notably MEMS vibrating gyroscopes, which are rotational inertial sensors. The applications of MEMS vibrating gyroscopes range from household appliances to GPS and even to military applications. However, the stability and reliability of these MEMS inertial sensors in space applications still pose challenges. In this research study, we introduce a simple design for a vibrating ring gyroscope with eight semicircular support springs connected to outside-placed anchors. The symmetric design structure with semicircular support springs provides higher sensitivity while minimizing mode mismatch. The design and modelling analysis of the vibrating ring gyroscope was conducted using Ansys 2023 R1. The proposed vibrating ring gyroscope has a ring radius of 1000 µm, a 210 µm radius for the semicircular support springs, a ring and support spring thicknesses of 10 µm, and an area of 80 × 80 µm^2 for the outside-placed anchors. The vibrating ring gyroscope operates at two identical elliptical-shape resonant modes, one for driving resonance frequency and the other for sensing resonance frequency. Both simulated resonance frequencies were measured at 48.78 kHz and 48.80 kHz. The modelled result achieved a mode mismatch of 0.02 kHz, which can be easily rectified with tuning electrodes.

Keywords: MEMS; vibrating ring gyroscope; mode matching; inertial sensor; IMU; ring resonator

Citation: Gill, W.A.; Howard, I.; Mazhar, I.; McKee, K. Simulation-Based Design and Analysis for MEMS Vibrating Ring Gyroscope. *Eng. Proc.* **2023**, *56*, 3. https://doi.org/10.3390/ASEC2023-15273

Academic Editor: Ana Paula Betencourt Martins Amaro

Published: 26 October 2023

1. Introduction

Microelectromechanical system (MEMS) vibrating gyroscopes are fundamental features of the inertial measurement unit (IMU) that have seen significant growth in their use in inertial sensor technology [1–4]. MEMS vibrating ring gyroscopes have been extensively discussed for research and development in space applications [5]. There are several other high-demand applications for MEMS vibrating ring gyroscopes in modern electronic systems. Inertial sensors based on MEMS vibrating gyroscopes have found widespread application in smartphones. They improve angular movement detection in digital cameras and have numerous other applications in fields as diverse as biomedical science, missile technology, and the transportation of microscale drug containers.

MEMS vibrating ring gyroscopes [6–11] are well suited for their use in IMU in space applications because of their symmetric design, high accuracy, mode matching, and robustness in severe environments [12–14]. The symmetric design structure of the ring-shaped gyroscope with semicircular springs allowed for the greater compliance required for harsh environments and high-intensity vibrations. In this study, we establish the simulation results of an internal ring MEMS vibrating ring gyroscope design. This paper discusses the design methodology, fabrication process, and preliminary design modelling of the vibrating ring gyroscope. The design modelling investigates the modal and harmonic analysis of the proposed vibrating ring gyroscope.

2. Fundamentals of MEMS Vibrating Ring Gyroscope

MEMS vibrating ring gyroscopes have two identical elliptical-shape vibrational modes: driving and sensing. In the case of MEMS vibrating ring gyroscopes, the ring serves as the proof mass "m" in a system with two axes of operation. The vibrating ring gyroscope operates by continually oscillating as an elliptical-mode shape along the drive axis. When the gyroscope is subjected to an external rotation, the primary oscillation starts to oscillate on the sensing axis as a secondary oscillation due to the Coriolis force effect. The direction of the secondary vibrational mode is the sensing axis. The vibrating ring gyroscope is schematically shown in Figure 1.

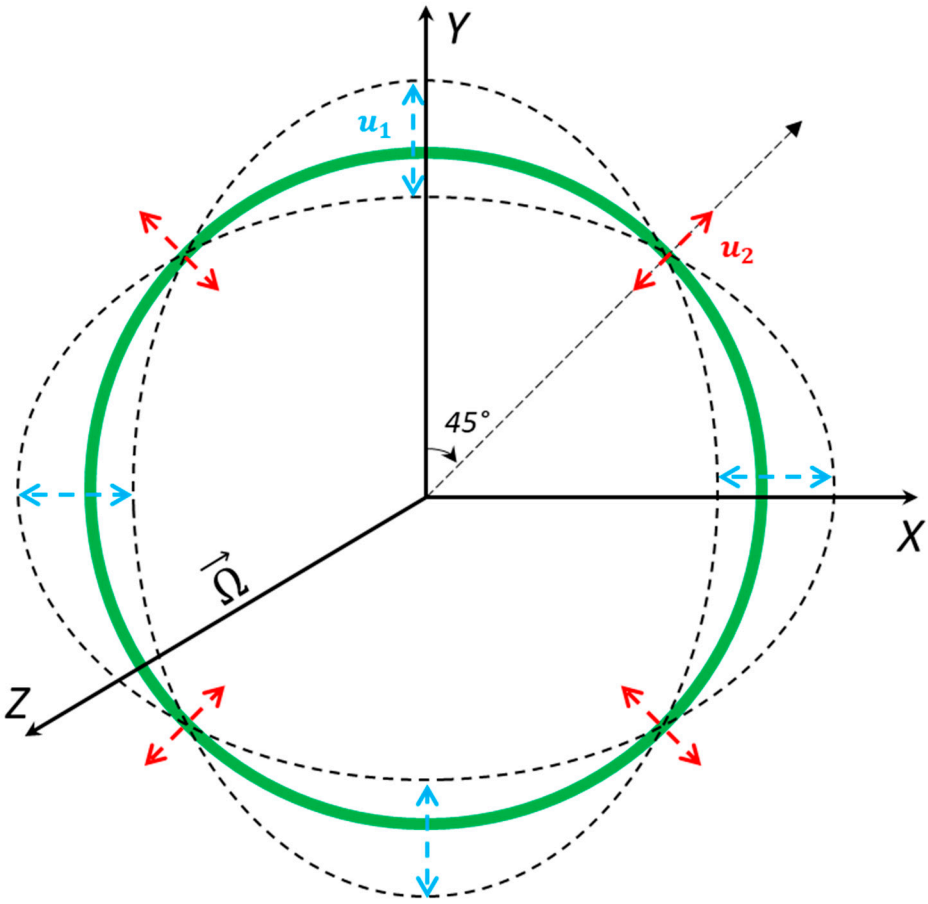

Figure 1. A schematic illustration of a resonating ring.

The fundamental equations of motion for a vibrating gyroscope are detailed below. Equation (1) is an equation for motion along the driving direction; Equation (2) is for motion along the sensing direction; and in Equation (3), we have the Coriolis force effect resulting from the external rotation and the driving oscillation. Here, "m" represents the ring mass, "c" the damping parameter, "k" the stiffness constant, "x" the driving axis displacement, "y" the sensing axis displacement, and "Ω" the external rotation. Here, we have the driving force F_d, the sensing force F_s, and the Coriolis force F_c.

$$m\frac{d^2x}{dt^2} + c\frac{dx}{dt} + kx = F_d \tag{1}$$

$$m\frac{d^2y}{dt^2} + c\frac{dy}{dt} + ky = F_s - F_c \tag{2}$$

$$F_C = -2m\Omega\frac{dx}{dt} \tag{3}$$

3. Design of MEMS Vibrating Ring Gyroscope

The design configuration of the MEMS vibrating ring gyroscope consisted of an internal ring resonator, eight support springs, and eight anchors in the gyroscope structure. The internal side of the eight semicircular springs is attached to the internal ring resonator. The outer side of the eight semicircular springs is attached to the eight outside-placed anchors. The anchors hold and support the whole gyroscope vibrational structure. A schematic diagram of the internal vibrating ring gyroscope is shown in Figure 2.

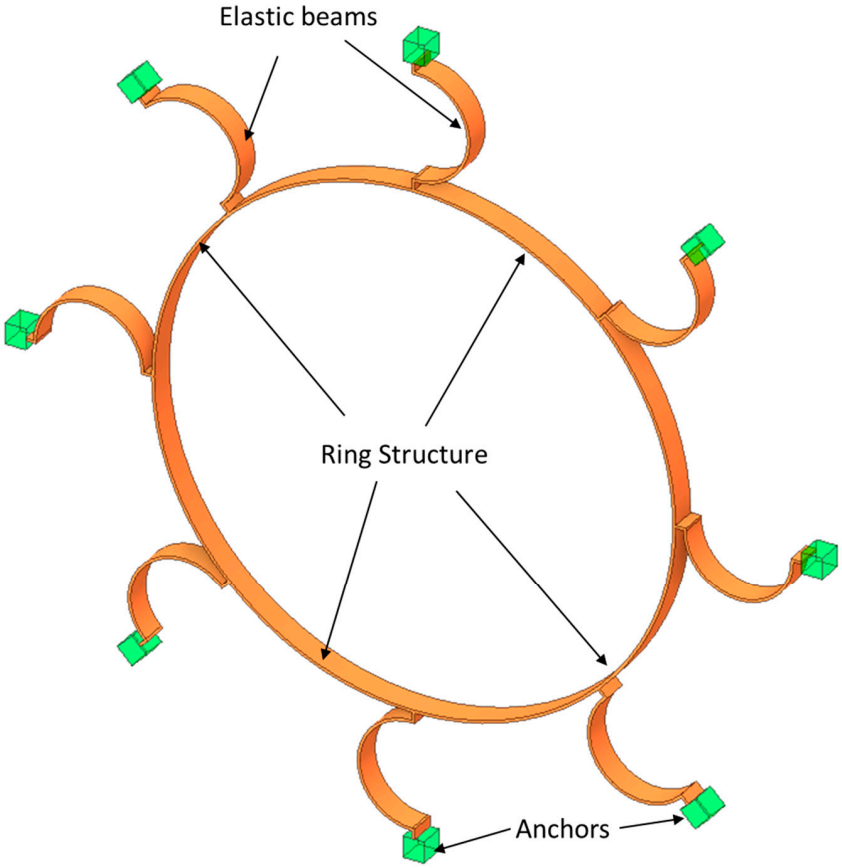

Figure 2. A schematic diagram of the internal ring vibrating gyroscope.

The semicircular springs in the vibrating ring gyroscope design are very effective energy absorbers, which makes them good candidates for space applications [15]. The compliance property of a semicircular spring refers to its ability to absorb energy at a certain rate. In challenging conditions, particularly characterized by intense shock or turbulence, it is essential for a gyroscope construction to possess a high level of robustness in order to effectively operate with increased sensitivity. The radius of the ring is 1000 μm, and the radius of the semicircular spring is 210 μm. The complete design components that make up the vibrating ring gyroscope are detailed in Table 1.

Table 1. Design components of a vibrating ring gyroscope.

Design Parameters	Value (μm)
Ring radius	1000
Structure height	100
Ring thickness	10
Semicircular spring radius	210
Semicircular spring thickness	10
Anchor area	80 × 80

The proposed fabrication process will be the silicon-on-insulator (SOI) process. The simple 4-mask design SOI microfabrication process introduced by the multi-user MEMS processes (SOIMUMPs) [16]. An overview of the microfabrication SOIMUMP for MEMS vibrating ring gyroscope steps is shown in Figure 3, and a description is provided below.

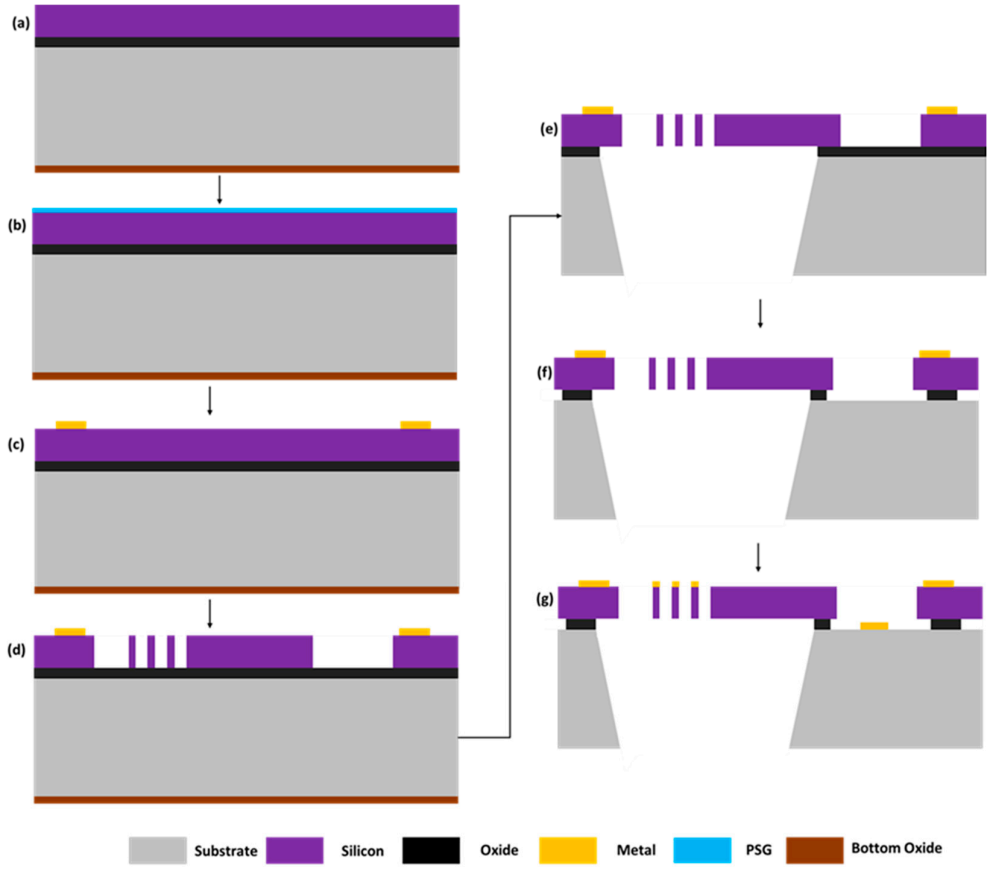

Figure 3. An overview of SOIMUMPs: (**a**) starting substrate SOI; (**b**) doped silicon with phosphosilicate glass (PSG); (**c**) development metal pads material; (**d**) silicon structural layer patterned; (**e**) etched with DRIE; (**f**) removal of exposed oxide layer; (**g**) metal deposited on the structural layer.

The SOI process starts with the defined thickness of the silicon on the insulator. The wafer comprises a 400 µm thick substrate and 1–2 µm thick oxide film with a 10 or 25 µm silicon structural layer. The bottom of the substrate is covered with the bottom oxide layer, as shown in the figure. The next step is doping the structural layer with the phosphossilicate glass (PSG) layer, which is performed by annealing at 1000 °C. After doping, the PSG layer is removed with chemical etching. The next step involves the development of the metal pad onto the structural layer. An electron beam evaporator is typically used for the deposition of metal stacks containing gold material in the nm range. The DRIE process is further used to etch the silicon structural layer to the bottom oxide layer. The oxide layer in the trench mask is removed with an oxide etching procedure. A silicon wafer is used to fabricate the shadow mask for the metal pattern. To reduce the risk of the shadow mask interfering with the patterned structures in the silicon layer of the SOI wafer, already existing standoffs are incorporated into the design of the shadow mask. Following the placement of the photoresist onto the shadow mask wafers, the next level of blanket metal undergoes lithographic patterning.

The shadow mask wafer undergoes a process of DRIE on silicon to achieve complete etching, resulting in the formation of through holes. These perforations through holes serve the purpose of facilitating the evaporation of metal. After that, the placement of the shadow mask is carried out, and it is temporarily bonded to the SOI wafer prior to the deposition of metal through an electron beam evaporator. The deposition of the blanket metal layer, consisting of chromium and gold, is limited to the through-hole regions of the

shadow mask. Following the process of sublimation, the shadow mask is subsequently eliminated. This results in the presence of a structured metal layer on the SOI wafer. The last step involves laser dicing and sorting out the final MEMS gyroscope chips.

4. Modelling Analysis

4.1. Modal Analsys

Modal analysis is a method that illustrates the fundamentals of vibrations based on the design structures. The natural frequency, vibration mode shape, and vibration stability are all analyzed in modal analysis. The ANSYS^{TM} software was used to carry out the preliminary design modelling of the proposed vibrating ring gyroscope. Figure 4 illustrates the vibration modes n = 1 and n = 2, respectively. The elliptical-mode shape of a vibrating ring gyroscope can be seen in the n = 1 in-plane flexural mode, and the triangle mode shape of a vibrating ring gyroscope can be seen in the n = 2 in-plane flexural mode. The resonance frequencies of the n = 1 flexural modes for driving and the sensing resonant frequencies were 48.78 kHz and 48.80 kHz, respectively. The mode mismatch between the driving and sensing frequencies was measured at 0.02 kHz. On the other side, for n = 2, the driving and sensing resonant frequencies were measured at high levels of 56.93 kHz and 56.94 kHz, respectively. The mode mismatch between the driving and sensing frequencies was measured at 0.01 kHz only.

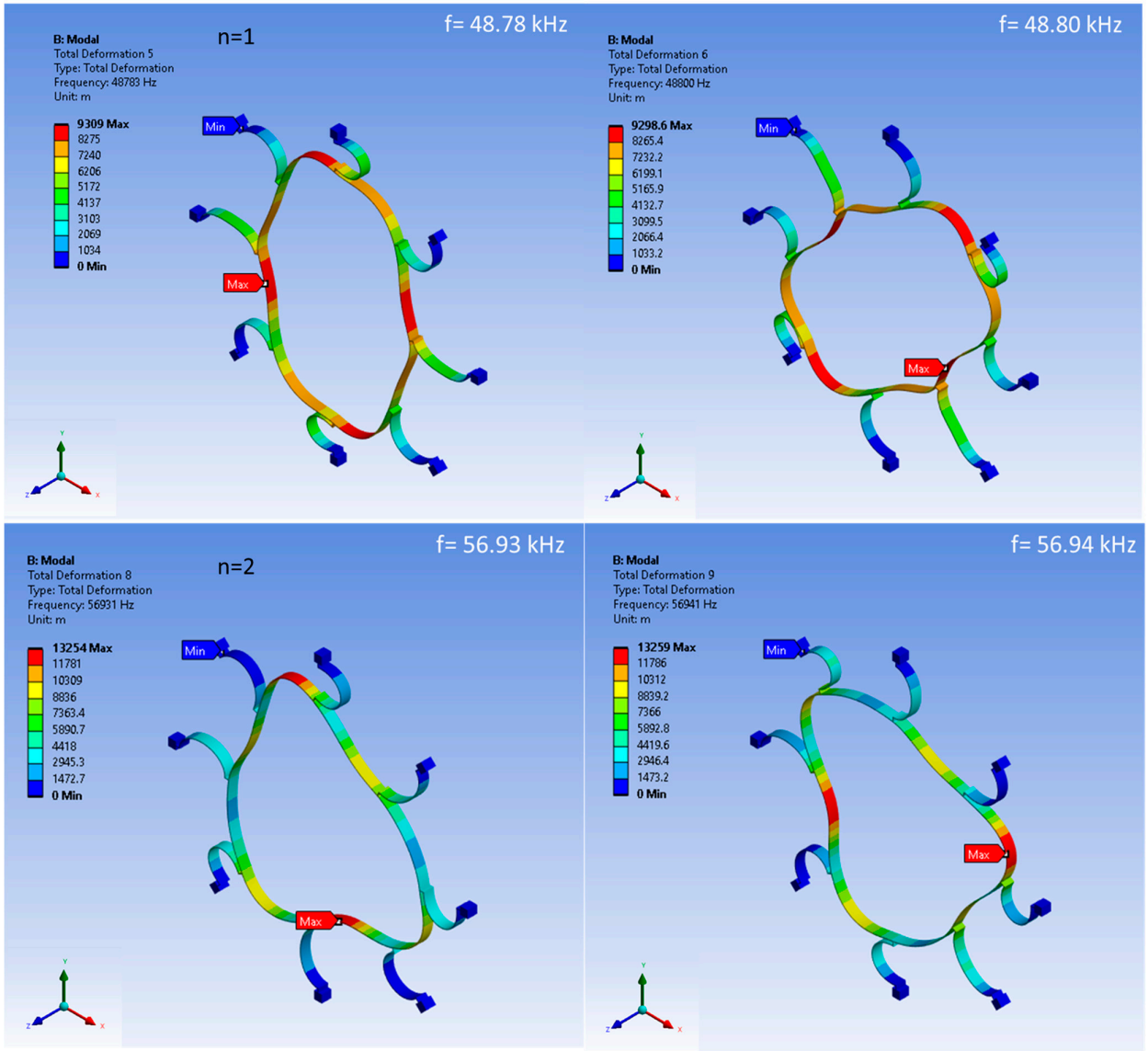

Figure 4. Modal analysis of a vibrating ring gyroscope for mode number n = 1 and n = 2.

4.2. Harmonic Analysis

An important aspect to investigate for the vibrating ring gyroscope is to evaluate the displacement response of the vibrating structure under the influence of electrostatic forces. The investigation of harmonic analysis is conducted using ANSYS^{TM} software in order to determine the frequency amplitude response of a structure under the influence of a certain perturbation force. Two separate peak values can be observed for the frequencies, corresponding to driving and sensing, respectively.

Thus, 0.5 µN of simple harmonic force is applied to the ring design in the directions of 0° and 180°. Figure 5 demonstrates the amplitude response subsequent to being applied to a harmonic force. A peak of resonance is seen at a frequency of 48.78 kHz, with a vibration amplitude of 1.3 µm in the driving axis.

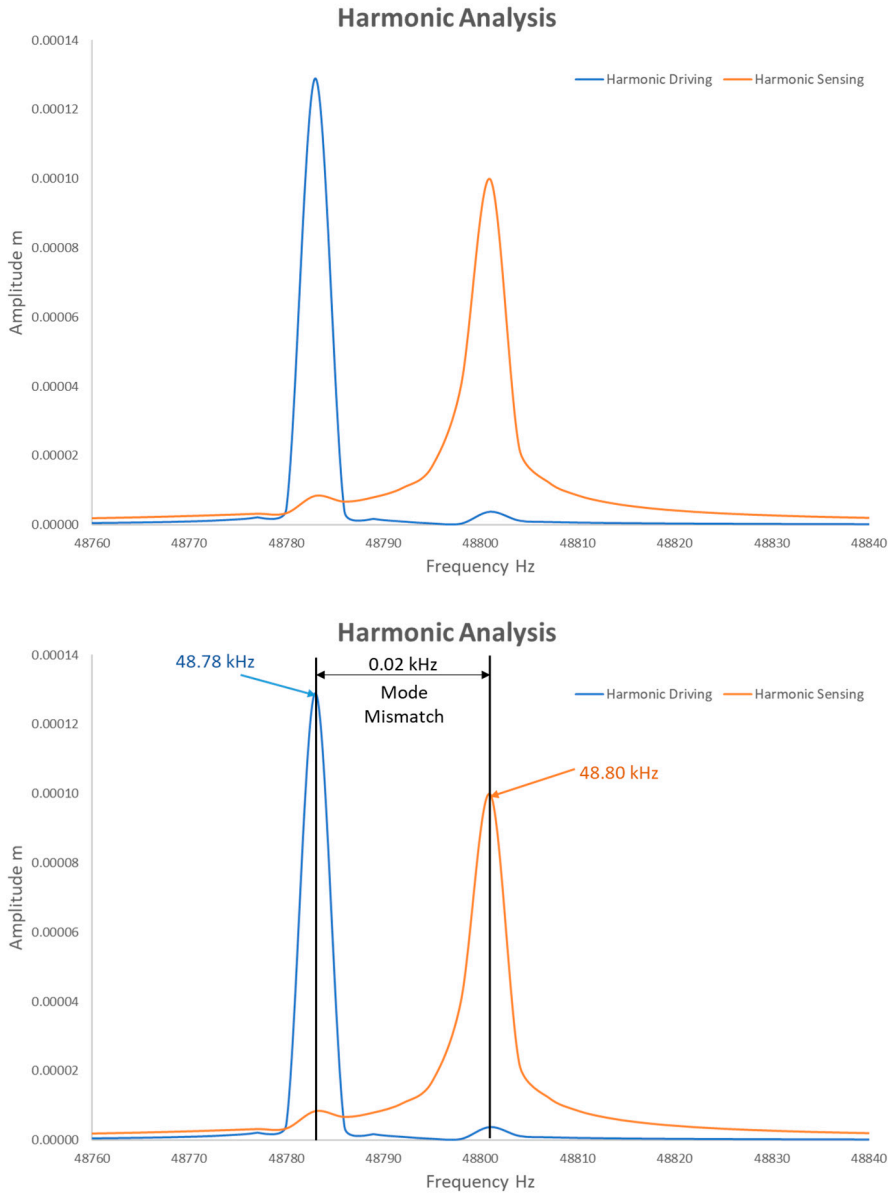

Figure 5. A harmonic analysis of vibrating ring gyroscope.

Further, the analysis focused on evaluating the harmonic response in the sensing direction with the continuous actuation force of 1 µN at angles of 45° and 225° in the sensing directions. Figure 5 demonstrates the observation of a resonant peak at a frequency of 48.80 kHz, showing an amplitude response of 0.9 µm in the sensing axis.

5. Conclusions

We were successful in developing a MEMS vibrating ring gyroscope with an internal ring structure design configuration. Higher compliance for high-shock settings is supported by the presence of internal ring resonators as well as a semicircular support spring configuration. The elliptical-shape mode frequencies of the vibrating ring gyroscope were determined to be 48.78 kHz for driving and 48.80 kHz for sensing. The ring radius of the gyroscope is 1000 µm. The difference in mode mismatch between the driving and sensing resonant frequencies was measured to be 0.02 kHz only. The drive amplitude with 1.3 µm is on the higher side, as compared to the sensing amplitude of 0.9 µm. The proposed vibrating ring gyroscope showed good initial results as a minimum mode mismatch of 0.02 kHz was modelled.

Author Contributions: The conceptualization was given by W.A.G. All the analyses, research, and construction of the figures were conducted by W.A.G. Writing: the manuscript was written by W.A.G. Writing (review and editing): the final manuscript was finished by I.H., I.M. and K.M. All authors have read and agreed to the published version of the manuscript.

Funding: This research received no external funding.

Institutional Review Board Statement: Not applicable.

Informed Consent Statement: Not applicable.

Data Availability Statement: All data are within this article.

Conflicts of Interest: The authors declare no conflict of interest.

References

1. Armenise, M.N.; Ciminelli, C.; Dell'Olio, F.; Passaro, V.M. *Advances in Gyroscope Technologies*; Springer Science & Business Media: New York, NY, USA, 2010.
2. Wu, X.; Xi, X.; Wu, Y.; Xiao, D. *Cylindrical Vibratory Gyroscope*; Springer: Berlin/Heidelberg, Germany, 2021.
3. Lee, J.S.; An, B.H.; Mansouri, M.; Al Yassi, H.; Taha, I.; Gill, W.A.; Choi, D.S. MEMS vibrating wheel on gimbal gyroscope with high scale factor. *Microsyst. Technol.* **2019**, *25*, 4645–4650. [CrossRef]
4. Passaro, V.M.N.; Cuccovillo, A.; Vaiani, L.; De Carlo, M.; Campanella, C.E. Gyroscope Technology and Applications: A Review in the Industrial Perspective. *Sensors* **2017**, *17*, 2284. [CrossRef] [PubMed]
5. Gill, W.A.; Ali, D.; An, B.H.; Syed, W.U.; Saeed, N.; Al-Shaibah, M.; Elfadel, I.M.; Al Dahmani, S.; Choi, D.S. MEMS multi-vibrating ring gyroscope for space applications. *Microsyst. Technol.* **2020**, *26*, 2527–2533. [CrossRef]
6. Ayazi, F.; Najafi, K. (Eds.) Design and fabrication of high-performance polysilicon vibrating ring gyroscope. In Proceedings of the IEEE Eleventh Annual International Workshop on Micro Electro Mechanical Systems An Investigation of Micro Structures, Sensors, Actuators, Machines and Systems, Heidelberg, Germany, 25–29 January 1998.
7. Ayazi, F.; Najafi, K. A HARPSS polysilicon vibrating ring gyroscope. *J. Microelectromech. Syst.* **2001**, *10*, 169–179. [CrossRef]
8. Cao, H.; Liu, Y.; Kou, Z.; Zhang, Y.; Shao, X.; Gao, J.; Huang, K.; Shi, Y.; Tang, J.; Shen, C.; et al. Design, fabrication and experiment of double U-beam MEMS vibration ring gyroscope. *Micromachines* **2019**, *10*, 186. [CrossRef] [PubMed]
9. Gill, W.A.; Howard, I.; Mazhar, I.; McKee, K. MEMS Vibrating Ring Gyroscope with Worm-Shaped Support Springs for Space Applications. *Eng. Proc.* **2022**, *31*, 2.
10. Syed, W.U.; An, B.H.; Gill, W.A.; Saeed, N.; Al-Shaibah, M.S.; Al Dahmani, S.; Choi, D.S.; Elfadel, I.A.M. Sensor Design Migration: The Case of a VRG. *IEEE Sens. J.* **2019**, *19*, 10336–10346. [CrossRef]
11. Hyun An, B.; Gill, W.A.; Lee, J.S.; Han, S.; Chang, H.K.; Chatterjee, A.N.; Choi, D.S. Micro-Electromechanical Vibrating Ring Gyroscope with Structural Mode-Matching in (100) Silicon. *Sens. Lett.* **2018**, *16*, 548–551. [CrossRef]
12. Yoon, S.W.; Lee, S.; Najafi, K. Vibration sensitivity analysis of MEMS vibratory ring gyroscopes. *Sens. Actuators A Phys.* **2011**, *171*, 163–177. [CrossRef]
13. Gill, W.A.; Howard, I.; Mazhar, I.; McKee, K. A Review of MEMS Vibrating Gyroscopes and Their Reliability Issues in Harsh Environments. *Sensors* **2022**, *22*, 7405. [CrossRef] [PubMed]
14. Liang, F.; Liang, D.-D.; Qian, Y.-J. Nonlinear Performance of MEMS Vibratory Ring Gyroscope. *Acta Mech. Solida Sin.* **2021**, *34*, 65–78. [CrossRef]

15. Gill, W.A.; Howard, I.; Mazhar, I.; McKee, K. Design and Considerations: Microelectromechanical System (MEMS) Vibrating Ring Resonator Gyroscopes. *Designs* **2023**, *7*, 106. [CrossRef]
16. Cowen, A.; Hames, G.; Monk, D.; Wilcenski, S.; Hardy, B. *SOIMUMPs Design Handbook*; Memscap Inc.: Durham, NC, USA, 2011; pp. 2002–2011.